

ICNMM2018-7721

MECHANISMS UNDERLYING FOAM-BASED ELECTRONUCLEATION OF HYDRATES

Palash V. Acharya

Department of Mechanical Engineering
The University of Texas at Austin
Austin, Texas, USA

Denise Lin

Department of Mechanical Engineering
The University of Texas at Austin
Austin, Texas, USA

Vaibhav Bahadur*

Department of Mechanical Engineering,
The University of Texas at Austin
Austin, Texas, USA

ABSTRACT

Nucleation of clathrate hydrates at low temperatures is constrained by very long induction (wait) times, which can range from hours to days. Electronucleation (application of an electrical potential difference across the hydrate forming solution) can significantly reduce the induction time. This work studies the use of porous open-cell foams of various materials as electronucleation electrodes. Experiments with tetrahydrofuran (THF) hydrates reveal that aluminum and carbon foam electrodes can enable voltage-dependent nucleation, with induction times dependent on the ionization tendency of the foam material. Furthermore, we observe a non-trivial dependence of the electronucleation parameters such as induction time and the recalescence temperature on the water:THF molar ratio. This study further corroborates previously developed hypotheses which associated rapid hydrate nucleation with the formation of metal-ion coordination compounds. Overall, this work studies various aspects of electronucleation with aluminum and carbon foams.

*Corresponding author: vb@austin.utexas.edu

INTRODUCTION

Clathrate hydrates [1, 2] are ice-like solids with a guest molecule (methane, carbon dioxide etc.) trapped in a lattice of water molecules. Many hydrates like CH₄ and CO₂ hydrates form under high pressure and low temperature conditions. Furthermore, it can take hours to days for hydrates to nucleate; this period is known as the thermodynamic induction time [3]. Induction times are especially high for quiescent systems,

which presents challenges for the development of many applications [4, 5], which require rapid hydrate formation (e.g. natural gas transportation by forming a hydrate). The use of surfactants and mechanical agitation of the precursor solution are common techniques to accelerate hydrate nucleation [6, 7].

The present group recently demonstrated the concept of electronucleation as a powerful tool to control and accelerate nucleation [10]. A significant reduction in the induction time for formation of tetrahydrofuran (THF) hydrates was observed upon the application of an electrical potential difference across a water:THF precursor solution, using cylindrical stainless steel electrodes. The induction time was voltage dependent, and was reduced to a few minutes at ~ 100 V.

It was further observed [11] that the use of aluminum foam open-cell electrodes reduced the induction times by 150X, when compared to bare stainless steel electrodes. Aluminum foams have been used for hydrate formation [12,13] to enable rapid removal of the heat generated during hydrate formation. The induction time with the use of such aluminum foam-based electrodes as anode was reduced to 10s of seconds (almost instantaneous nucleation) at low voltages (~20 V). Electronucleation was seen to depend strongly on the polarity of the foam electrode. Two mechanisms were proposed to explain accelerated nucleation, namely electrolytic bubble generation (when the aluminum foam is the cathode), and the formation of aluminum-based coordination compounds in solution (when the aluminum foam is the anode).

In this work, we further study foam-based electronucleation via the use of carbon foams. We also experimentally uncover the influence of various experimental parameters such as the foam material, water:THF molar ratio, and foam porosity on the induction time and recalescence temperature. The hypothesis being explored in this work is that electrode materials with a high ionization tendency will enable faster nucleation, when used as the anode.

EXPERIMENTAL SETUP AND PROCEDURES

THF hydrates were used in this study as a substitute for methane hydrates [14-17]. THF hydrates are formed from a water-THF mixture (stoichiometric molar ratio is (water:THF ~17:1)) at atmospheric pressure, and below 4.4 °C. In this study the molar ratio was varied from 10:1 to 20:1 to simulate conditions where the ratio of water and THF will not be the stoichiometric value.

The experimental setup used in this study is detailed in Figure 1. The THF:water mixture was contained in a test tube (diameter : 14mm), which was fitted with rubber stoppers. The stopper were fitted with a T-type ungrounded thermocouple and the electrodes, which were immersed in the solution. These tubes were cooled in an isothermal cooling bath filled with a 50/50 mixture of ethylene glycol and water. The temperature and the current passing through the precursor solution was monitored, and used to detect nucleation.

A 6 x 8 x 50 mm sized foam plug was used as the electronucleation electrode, in line with our previous study [11]. A cylindrical stainless steel electrode was used as the other electrode, with the spacing between the electrodes and thermocouples being 5mm. These electrodes were connected to a DC power supply and an ammeter.

Open-cell aluminum foams having the following specifications were used as the baseline electrodes: porosity of 92%, 20 pores per inch (PPI), and a surface area to volume ratio of 1720 m²/m³. Open-cell carbon foams had the following specifications: porosity 97%, 30 pores per inch (PPI), and a surface area to volume ratio of 1722 m²/m³.

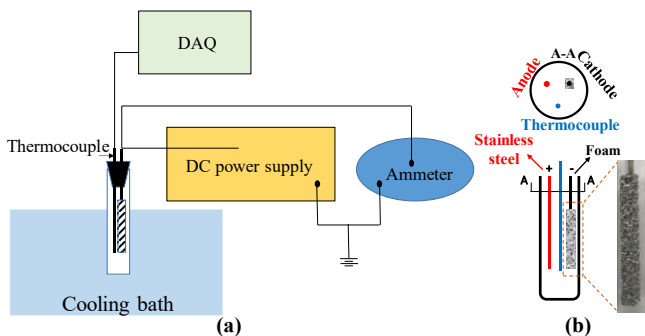


Figure 1. (a) Schematic of experimental setup, (b) Stainless steel and aluminum foam electrodes inside the tube with hydrate forming solution.

The test tube containing the precursor solution was initially agitated to ensure complete miscibility and then degassed for 10 minutes in a sonication bath to remove dissolved gas. Dissolved gas bubbles can act as nucleation sites via bubble cavitation events. The degassed solution was then immersed in the cooling bath and the temperature was lowered to -5 °C. Once the contents of the tube reached a steady state temperature of -5 °C, a DC electrical voltage was applied. The induction time was measured from this point onwards to the onset of hydrate nucleation.

Nucleation was detected by tracking the thermal signature of the solution, as detailed in our previous studies [10, 11]. The heat released at the onset of nucleation instantaneously raises the temperature of the solution to ~ 4 °C (Figure 2), this is known as recalescence. Another indication [10] of hydrate nucleation is a sudden decrease in the electrical conductivity due to the formation of hydrates (Figure 2). Similar techniques have previously been used to infer nucleation of THF hydrates [19] and ice [20-22].

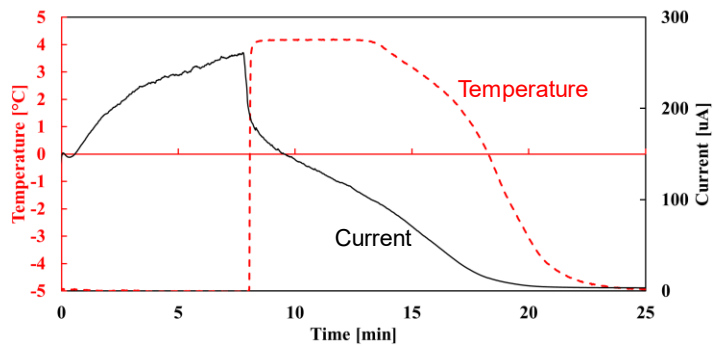


Figure 2. Temperature and current flow in the hydrate forming solution. The onset of nucleation is indicated by a sudden temperature spike along with a simultaneous decrease in current.

Before discussing the results obtained from the present experiments, it is helpful to briefly summarize the two polarity-dependent mechanism responsible for electronucleation, as discussed in our previous work [10,11].

When the metal foam is the cathode, water is reduced to hydroxyl ions, thereby generating hydrogen gas, which can be observed as bubbles at the cathode ($4\text{H}_2\text{O} + 4\text{e}^- \rightarrow 4\text{OH}^- + 2\text{H}_2\uparrow$). These bubbles act as nucleation sites, and phenomena like bubble growth or detachment can trigger nucleation. However, when the foam is the anode, oxidation of the foam material is favored over that of hydroxyl ions; this causes the foam material to enter the solution as positive ions (eg. Al^{3+}) [11, 23-26]. Hydrolysis of these ions leads to the formation of coordination compounds. The resemblance of these compounds to the structure of hydrates is hypothesized to be responsible for hydrate nucleation [11].

RESULTS AND DISCUSSIONS

Influence of foam electrode material on electronucleation

THF hydrate nucleation experiments were conducted with reticulated vitreous carbon foam as the electronucleation electrode. The objective of these experiments was to further validate the proposed hypotheses related to the importance of electrode materials in electronucleation. The data points in the following results are the average of more than five individual measurements.

Table 1 shows that the induction time for a carbon foam cathode is very similar to that of an aluminum foam cathode. This is a very significant finding and confirms the hypothesis that bubble related mechanistic effects influence electronucleation. These mechanistic effects are independent of the electrode material, and the electronucleation tendency is therefore expected to show material invariance. The present findings clearly support this hypothesis.

In contrast, when the foam is used as the anode, there is a 10X difference in the induction times associated with carbon and aluminum electrodes. Aluminum foams electronucleate much faster than carbon foams, when used as the anode. The influence of electrode material on electronucleation is thus clearly outlined via these experiments. The tendency of a metal to undergo oxidation is quantified by its electronegativity; lower electronegativity implies a higher tendency to oxidize. The electronegativity of carbon and aluminum on a Pauling scale are 2.55 and 1.61 respectively, which implies that carbon has a significantly lower tendency to ionize and enter the precursor solution as ions. On the other hand, aluminum ions enter the solution readily (as detected in [11]), and the formation of aluminum-based coordination compounds can trigger rapid electronucleation. Overall, the experiments with carbon foams provide additional validation of the hypotheses on the mechanisms underlying electronucleation.

Table 1. Measured induction times for aluminum and carbon foams.

	Induction time (minutes) at 20 V			
	Foam as cathode		Foam as anode	
	Carbon foam	Al foam	Carbon foam	Al foam
Average	2.43	2.16	3.57	0.31
Standard deviation	0.86	0.29	1.7	0.08

Influence of molar composition of precursor solution on electronucleation

The influence of the water:THF molar ratio on induction time with aluminum foams is shown in Table 2. The electronucleation voltage in all these experiments was 20 V. It is seen that the induction time decreases (from ~5.6 to ~1.55 minutes) as the relative fraction of water is increased. Expedited nucleation in the presence of a higher water fractions

can be explained by examining the structure of THF hydrates. THF molecules (C_4H_8O) form structure II hydrates, wherein the THF molecules are encased in the cavities within the cage structure formed by the water molecules. The presence of a relatively larger number of water molecules will increase the probability that THF molecules will find a cage structure with an empty cavity, which should translate to faster nucleation. Also, for high water fractions the probability of ice nucleation also increases, which in turn can trigger hydrate nucleation (since hydrates have similar structure as ice). Overall, these results suggest that water rich solutions will trigger faster hydrate nucleation.

Table 2. Measured induction times for different molar ratios of water: THF.

Molar ratio	Induction time (minutes) at 20 V		
	10:1	15:1	20:1
Average	5.59	2.16	1.56
Standard deviation	0.99	0.29	0.59

To understand nucleation in more detail, the recalescence temperature was also monitored. The recalescence temperature for various molar ratios is shown in Table 3. The average recalescence temperature at a molar ratio of 15:1 (close to stoichiometric ratio) is 4.16 °C which is in line with our previous results [10,11]. However, it is observed that a deviation from this molar ratio of 15:1 results in a drop in the recalescence temperature. Similar results were obtained by Dai et al. [19] wherein it was reported that any deviation from the stoichiometric ratio reduced the recalescence temperature. The lower temperature for a water-rich molar ratio of 20:1 could be explained by the simultaneous formation of ice (which has a recalescence temperature of 0 °C). This ice formation can trigger hydrate nucleation, which explains the low induction times in Table 2. The mechanisms underlying the reduced recalescence temperatures for hydrate-rich solutions (molar ratio of 10:1) is not clear from the present experiments. Overall, it is seen that the recalescence temperature reduces from the thermodynamic value as the relative concentrations deviate from the stoichiometric value.

Table 3. Recalescence temperatures for different molar ratios of water: THF.

Molar ratio	Recalescence temperature (°C) at 20 Volts		
	10:1	15:1	20:1
Average	2.05	4.16	2.8
Stdev	0.56	0.04	0.27

Electronucleation with aluminum foam cathodes

In our previous study [11], it was observed that the use of aluminum foams as the anode led to lower induction times compared to aluminum foam cathodes. In order to further quantify the benefits of aluminum foam anodes, experiments were conducted with the foam used as the cathode to estimate the higher voltages at which the induction times would be similar to that of foam anodes. Table 4 summarizes key results from our previous work [11], and the present experiments at higher voltages.

Table 4. Induction time for THF hydrate nucleation (minutes).

Previous study [11]	Al foam as cathode				Al foam as anode			
	20	10	5	0	20	10	5	0
Voltage (V)	20	10	5	0	20	10	5	0
Average	2.1	10.2	62	>12 hours	0.3	0.7	1.6	>12 hours
Standard deviation	0.3	1.9	7	-	0.1	0.16	0.3	-

Current work	Al foam as cathode	
Voltage (V)	50	80
Average	0.59	0.35
Standard deviation	0.2	0.18

The results in Table 4 suggest that in order to achieve the same induction time, aluminum foam cathodes will require 4X the voltage (~ 80 V) required with aluminum foam anodes (~ 20V). These experiments clearly show that the influence of polarity is significant, and that the appropriate polarity can significantly reduce induction time or supercooling requirements.

Influence of foam porosity on electronucleation

Experiments were also conducted with an aluminum foam having a different porosity than the baseline foam. The second foam had a PPI of 10 and a surface area to volume ratio of 790 m²/m³. Experiments were conducted with these foams as the cathode. For such a configuration, nucleation is expected to be controlled by the mechanistic effects associated with electrolytic bubble generation. Table 5 shows that the induction time decreases as the porosity decreases. A likely explanation is that as the surface area to volume ratio decreases, it concentrates the current flowing through the solution to a smaller surface area, thereby increasing the local concentration of bubbles, which promote faster nucleation.

Table 5. Measured induction times for different foam porosities.

Pores per inch	Induction time (minutes) @20V	
	20	10
Average	2.16	0.81
Standard deviation	0.29	0.28

CONCLUSIONS

This work presents additional experimental investigations to understand various aspects of metal foam-based electronucleation of hydrates. Experiments with different foam materials (aluminum, carbon) clearly confirm the hypothesis that two mechanisms are at play. The influence of varying molar concentrations and foam porosities is also quantified via experiments. Overall, it is seen that electrode material, polarity and the composition of the precursor solution are important parameters in determining the electronucleation kinetics of hydrates.

ACKNOWLEDGEMENTS

The authors acknowledge American Chemical Society Petroleum Research Fund PRF 54706- DNI5, Welch Foundation Grant # F-1837 and National Science Foundation CBET-1653412 for supporting this work.

REFERENCES

- (1) Eslamimanesh, A.; Mohammadi, A. H.; Richon, D.; Naidoo, P.; Ramjugernath, D. Application of Gas Hydrate Formation in Separation Processes: A Review of Experimental Studies. *J. Chem. Thermodyn.* 2012, 46, 62–71.
- (2) Veluswamy, H. P.; Kumar, R.; Linga, P. Hydrogen Storage in Clathrate Hydrates: Current State of the Art and Future Directions. *Appl. Energy* 2014, 122, 112–132.
- (3) Sloan, E.D. and Koh, C.A., Clathrate Hydrates of Natural Gases Third Edition. CRC Press, 2008, 119.
- (4) Sum, A. K.; Koh, C. A.; Sloan, E. D. Clathrate Hydrates: From Laboratory Science to Engineering Practice. *Ind. Eng. Chem. Res.* 2009, 48 (16), 7457–7465.
- (5) Chatti, I.; Delahaye, A.; Fournaison, L.; Petitet, J. P. Benefits and Drawbacks of Clathrate Hydrates: A Review of Their Areas of Interest. *Energy Convers. Manag.* 2004, 46, 1333–134.
- (6) Zhong, Y.; Rogers, R. E. Surfactant Effects on Gas Hydrate Formation. *Chem. Eng. Sci.* 2000, 55, 4175–4187.
- (7) Zhang, J. S.; Lee, S.; Lee, J. W. Kinetics of Methane Hydrate Formation from SDS Solution. *Ind. Eng.*

- Chem. Res. **2007**, 46, 6353–6359.
- (8) Ganji, H.; Manteghian, M.; Sadaghiani zadeh, K.; Omidkhah, M. R.; Rahimi Mofrad, H. Effect of Different Surfactants on Methane Hydrate Formation Rate, Stability and Storage Capacity. *Fuel* **2007**, 86, 434–441.
 - (9) Ando, N.; Kuwabara, Y.; Mori, Y. H. Surfactant Effects on Hydrate Formation in an Unstirred Gas/liquid System: An Experimental Study Using Methane and Micelle-Forming Surfactants. *Chem. Eng. Sci.* **2012**, 73, 79–85.
 - (10) Carpenter K.; Bahadur V.; Electronucleation for rapid and controlled formation of hydrates. *J. Phys. Chem. Lett.*, **2016** , 7(13) , 2465-2469
 - (11) Shahriari A, Acharya PV, Carpenter K, Bahadur V, *Langmuir* **2017**; 33(23): 5652-5656.
 - (12) Yang L.; Fan S.S.; Wang Y.H.; Lang X.M; Xie D.L. Accelerated formation of methane hydrate in aluminum foam. *Ind. Eng. Chem.*, **2011** , 50 , 11563-11569.
 - (13) Fan, S., Yang, L., Lang, X., Wang, Y., and Xie, D., 2012, “Kinetics and thermal analysis of methane hydrate formation in aluminum foam,” *Chem. Eng. Sci.*, 82, pp. 185–193
 - (14) Wilson, P. W.; Lester, D.; Haymet, a. D. J. Heterogeneous Nucleation of Clathrates from Supercooled Tetrahydrofuran (THF)/water Mixtures, and the Effect of an Added Catalyst. *Chem. Eng. Sci.* **2005**, 60, 2937–2941.
 - (15) Zhang, J. S.; Lo, C.; Somasundaran, P.; Lu, S.; Couzis, A.; Lee, J. W. Adsorption of Sodium Dodecyl Sulfate at THF Hydrate / Liquid Interface. *J. Phys. Chem.* **2008**, 112, 12381–12385.
 - (16) Liu, W.; Wang, S.; Yang, M.; Song, Y.; Wang, S.; Zhao, J. Investigation of the Induction Time for THF Hydrate Formation in Porous Media. *J. Nat. Gas Sci. Eng.* **2015**, 24, 357–364.
 - (17) Wilson, P. W.; Haymet, A. D. J. Hydrate Formation and Re-Formation in Nucleating THF/water Mixtures Show No Evidence to Support a “Memory” Effect. *Chem. Eng. J.* **2010**, 161, 146–150.
 - (18) Tombari, E.; Presto, S.; Salvetti, G.; Johari, G. P. Heat Capacity of Tetrahydrofuran Clathrate Hydrate and of Its Components, and the Clathrate Formation from Supercooled Melt. *J. Chem. Phys.* **2006**, 124, 154507–154506.
 - (19) Dai, S.; Lee, J. Y.; Santamarina, J. C. Hydrate Nucleation in Quiescent and Dynamic Conditions. *Fluid Phase Equilib.* **2014**, 378, 107–112.
 - (20) Bauerecker, S.; Ulbig, P.; Buch, V.; Vrbka, L.; Jungwirth, P. Monitoring Ice Nucleation in Pure and Salty Water via High-Speed Imaging and Computer Simulations. *J. Phys. Chem. C* **2008**, 167, 7631–7636.
 - (21) Alizadeh, A.; Yamada, M.; Li, R.; Shang, W.; Otta, S.; Zhong, S.; Ge, L.; Dhinojwala, A.; Conway, K. R.; Bahadur, V.; et al. Dynamics of Ice Nucleation on Water Repellent Surfaces. *Langmuir* **2012**, 28 , 3180–3186.
 - (22) Carpenter, K.; Bahadur, V. Electrofreezing of Water Droplets under Electrowetting Fields. *Langmuir* **2015**, 31, 2243–2248.
 - (23) Hozumi T.; Saito A.; Okawa S.; Watanabe K. Effects of electrode materials on freezing of supercooled water in electric freeze control. *Int. J. Refrig.*, **2003**, 26, 537-542.
 - (24) Shichiri T.; Nagata T. Effect of Electric currents on the nucleation of ice crystals in the melt. *J. Cryst. Growth*, **1981**, 54 ,207-210
 - (25) Orłowska M.; Havet M; Le-Bail A. Controlled ice nucleation under high voltage DC Electrostatic field conditions. *FoodRes. Int.*, **2009** , 42(7), 879-884.
 - (26) Wei S.; Xiaobin X.; Hong Z.; Chuanxiang X. Effect of dipole polarization of water molecules on ice formation under an electrostatic field. *Cryobiology*, **2008**, 56, 93-99.s